

# Decay of symmetry protected quantum states

Anna A. Bychek<sup>1</sup>, Dmitrii N. Maksimov<sup>1,2</sup>, and Andrey R. Kolovsky<sup>1,2</sup>

<sup>1</sup>*LV Kirensky Institute of Physics, Federal Research*

*Center KSC SB RAS, 660036, Krasnoyarsk, Russia*

<sup>2</sup>*Siberian Federal University, Krasnoyarsk, 660041, Russia*

(Dated: January 28, 2021)

# Abstract

We study the decay of bosonic many-body states in the three well Bose-Hubbard chain where bosons in the central well can escape into a reservoir. For vanishing inter-particle interaction this system supports a non-decaying many-body state which is the antisymmetric Bose-Einstein condensate with particles occupying only the edge wells. In the classical approach this quantum state corresponds to a symmetry protected non-decaying state which is stable even at finite interaction below a certain intensity threshold. Here we demonstrate that despite the classical counterpart is stable the antisymmetric Bose-Einstein condensate is always metastable at finite interatomic interactions due to quantum fluctuations.

## I. INTRODUCTION

Dissipative quantum systems are of a large importance as they pave a way for manipulating quantum matter for preparation of pure [1] as well as highly entangled [2] states, and implementation of quantum computations [3]. One particular example of dissipative quantum systems realized with cold atoms are open systems which can exchange particles with a reservoir [4–10], so, neither the energy nor the particle number is preserved. When an open system is coupled with two reservoirs with different chemical potentials, it realizes an atomtronic analogue [11] of semiconductor devices [7, 9, 10, 12, 13]. Alternatively a quantum lattice system can be coupled with the environment only in a single lattice site as experimentally demonstrated in [14].

Here we consider decay of Bose particles from a triple quantum well with the central well coupled to environment, i.e. the bosonic particles are drained into a reservoir [15]. Despite its simplicity the three site-model BH does not allow for exact analytic solution [15–19]. In this paper we employ pseudoclassical approach [20–28] which allows us to cast the problem into a form of coupled driven nonlinear oscillators. From the pure classical perspective this system supports a non-decaying solution with equal intensities but opposite phases on the edge sites. Such a solution has a zero amplitude at the central site, and, therefore, is not directly coupled to the reservoir. This kind of localized solution, existing in the system despite the loss channels is allowed, is known as a bound state in the continuum (BIC) [29]. In particular, the BIC to be considered in the present work is analogous to that supported by a pair of side-defects coupled to photonic crystalline waveguides [30, 31]. From the quantum

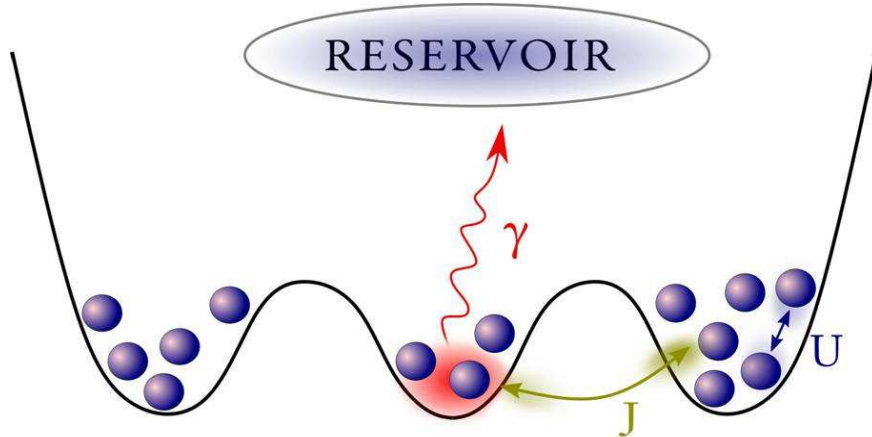


FIG. 1. Sketch of the system.

mechanical perspective the discussed BIC is the antisymmetric Bose-Einstein condensate (BEC) with particles occupying only the edge sites. The central problem to be addressed in the work is the account of the inter-particle interaction. We shall examine the stability of non-linear BIC in the classical regime and investigate the link between the classical and quantum solutions. It shall be demonstrated that even a classically stable nonlinear BIC undergoes a slow rate decay due to quantum fluctuations. Thus, the antisymmetric BEC is always a metastable state. We shall show that the quantum fluctuations can be accurately described within the pseudoclassical framework by the stochastic force emerging in the nonlinear coupled oscillator model.

## II. MASTER EQUATION AND PSEUDOCCLASSICAL APPROACH

We consider a linear trimer of three coupled potential wells. The trimer is initially occupied by  $N_0$  bosons which can tunnel between the wells as shown in Fig. 1. The tunnelling dynamics is controlled by the Bose-Hubbard Hamiltonian

$$\hat{\mathcal{H}} = -\frac{J}{2} \sum_{\ell=1}^2 \left( \hat{a}_{\ell+1}^\dagger \hat{a}_\ell + \text{h.c.} \right) + \frac{U}{2} \sum_{\ell=1}^3 \hat{n}_\ell (\hat{n}_\ell - 1), \quad (1)$$

where  $\hat{a}_\ell^\dagger$  ( $\hat{a}_\ell$ ) is the creation (annihilation) operator at the  $\ell_{\text{th}}$  site,  $\hat{n}_\ell$  is the number operator at the  $\ell_{\text{th}}$  site,  $J$  is the interwell tunnelling rate and  $U$  is the interaction constant. By now the BH model has grown to one of the seminal model in physics of cold atoms which scopes quantum phase transitions [32], the effects of Josephson oscillations [33, 34], atomic Bloch

oscillations [35, 36], refill dynamics in the presence of induced losses, [14, 37], spontaneous breaking of the symmetry [38], and quantized current in the engineered transport channel [7, 9, 10] to mention a few results relevant to the present paper. Here, following [15], we assume that the central well is attached to an atom sink as shown in Fig. 1. Then the system dynamics is described by the density matrix  $\widehat{\mathcal{R}}$  which obeys the master equation

$$\frac{\partial \widehat{\mathcal{R}}}{\partial t} = -i[\widehat{\mathcal{H}}, \widehat{\mathcal{R}}] + \widehat{\mathcal{L}}(\widehat{\mathcal{R}}) \quad (2)$$

with the loss operator of a Lindblad form

$$\widehat{\mathcal{L}}(\widehat{\mathcal{R}}) = -\frac{\gamma}{2} \left( \hat{a}_2^\dagger \hat{a}_2 \widehat{\mathcal{R}} - 2\hat{a}_2 \widehat{\mathcal{R}} \hat{a}_2^\dagger + \widehat{\mathcal{R}} \hat{a}_2^\dagger \hat{a}_2 \right), \quad (3)$$

where  $\gamma$  is the loss rate.

The pseudoclassical approach is introduced by replacing each operator  $\widehat{A}$  by its Weyl symbol which is a function on the phase space [39],

$$\text{symb}[\widehat{A}] = A(a, a^*), \quad (4)$$

with  $a, a^*$  as the complex conjugated canonical variables defined as the Weyl symbols of the annihilation and creation operators

$$\text{symb}[\hat{a}] = a, \quad \text{symb}[\hat{a}^\dagger] = a^*, \quad (5)$$

where we omitted the subindex  $\ell$  for simplicity. The Weyl symbols of an operator product of two operators are computed via the Moyal star product of the Weyl symbols of the two operators

$$A \star B = A \exp \left[ \frac{\hbar}{2} \left( \frac{\partial^{\leftarrow}}{\partial a} \frac{\partial^{\rightarrow}}{\partial a^*} - \frac{\partial^{\leftarrow}}{\partial a^*} \frac{\partial^{\rightarrow}}{\partial a} \right) \right] B. \quad (6)$$

For instance, it is easy to see from Eq. (6) that the Weil symbol of the number operator is

$$\text{symb}[\hat{n}] = a^* \star a = |a|^2 - \frac{1}{2}. \quad (7)$$

The figure of merit in the pseudoclassical approach is the Weyl symbol of the density matrix known as the Wigner function

$$\mathcal{W} = \text{symb}[\widehat{\mathcal{R}}]. \quad (8)$$

Applying Eq. (6) to the master equation, Eq. (2) one finds that the Wigner function obeys the following equation [40, 41]

$$\begin{aligned}
\frac{\partial \mathcal{W}}{\partial t} = & -i \sum_{\ell=1}^3 \left[ U (1 - |\alpha_\ell^2|) \left( \alpha_\ell \frac{\partial \mathcal{W}}{\partial \alpha_\ell} - \alpha_\ell^* \frac{\partial \mathcal{W}}{\partial \alpha_\ell^*} \right) - \frac{U}{4} \left( \frac{\partial^3 \alpha_\ell^* \mathcal{W}}{\partial \alpha_\ell \partial \alpha_\ell^2} - \frac{\partial^3 \alpha_\ell \mathcal{W}}{\partial \alpha_\ell^2 \partial \alpha_\ell^*} \right) \right] \\
& - i \frac{J}{2} \sum_{\ell=1}^2 \left( \alpha_{\ell+1} \frac{\partial \mathcal{W}}{\partial \alpha_\ell} + \alpha_\ell \frac{\partial \mathcal{W}}{\partial \alpha_{\ell+1}} - \alpha_{\ell+1}^* \frac{\partial \mathcal{W}}{\partial \alpha_\ell^*} - \alpha_\ell^* \frac{\partial \mathcal{W}}{\partial \alpha_{\ell+1}^*} \right) \\
& + \frac{\gamma}{2} \left( \alpha_2 \frac{\partial \mathcal{W}}{\partial \alpha_2} + 2\mathcal{W} + \alpha_2^* \frac{\partial \mathcal{W}}{\partial \alpha_2^*} \right) + \frac{\gamma}{2} \frac{\partial^2 \mathcal{W}}{\partial \alpha_2 \partial \alpha_2^*}. \tag{9}
\end{aligned}$$

The above equation contains third order derivatives which do not allow to interpret it as a Fokker-Plank equation with a positive definite or positive semidefinite diffusion matrix [40].

The pseudoclassical limit of Eq. (9) is obtained by setting  $N_0 \rightarrow \infty$  while keeping  $g = UN_0 = \text{Const}$ . In what follows the quantity  $g$  will be referred to as the macroscopic interaction constant. Let us apply the following substitution

$$\alpha_\ell = \sqrt{N_0} a_\ell, \quad \alpha_\ell^* = \sqrt{N_0} a_\ell^*. \tag{10}$$

Then Eq. (9) transforms to

$$\begin{aligned}
\frac{\partial \mathcal{W}}{\partial t} = & -i \sum_{\ell=1}^3 \left[ g \left( \frac{1}{N_0} - |a_\ell^2| \right) \left( a_\ell \frac{\partial \mathcal{W}}{\partial a_\ell} - a_\ell^* \frac{\partial \mathcal{W}}{\partial a_\ell^*} \right) \right] \\
& - i \frac{J}{2} \sum_{\ell=1}^2 \left( a_{\ell+1} \frac{\partial \mathcal{W}}{\partial a_\ell} + a_\ell \frac{\partial \mathcal{W}}{\partial a_{\ell+1}} - a_{\ell+1}^* \frac{\partial \mathcal{W}}{\partial a_\ell^*} - a_\ell^* \frac{\partial \mathcal{W}}{\partial a_{\ell+1}^*} \right) \\
& + \frac{\gamma}{2} \left( a_2 \frac{\partial \mathcal{W}}{\partial a_2} + 2\mathcal{W} + a_2^* \frac{\partial \mathcal{W}}{\partial a_2^*} \right) + \frac{\gamma}{2N_0} \frac{\partial^2 \mathcal{W}}{\partial a_2 \partial a_2^*} + \mathcal{O}(N_0^{-2}). \tag{11}
\end{aligned}$$

Neglecting  $\mathcal{O}(N_0^{-2})$  term we arrive at a true Fokker-Plank equation where the first term in the third line can be viewed as dissipation while the second term in the same line is diffusion [27, 28].

The dynamics under the Fokker-Planck equation, Eq. (11) can be unravelled into a set of dissipative Langevin equations

$$\begin{aligned}
ida_1 &= \left( -\frac{J}{2} a_2 + g |a_1|^2 a_1 \right) dt, \\
ida_2 &= \left[ -\frac{J}{2} (a_1 + a_3) + g |a_2|^2 a_2 - i \frac{\gamma}{2} a_2 \right] dt + \sqrt{\frac{\gamma}{2N_0}} d\xi, \\
ida_3 &= \left( -\frac{J}{2} a_2 + g |a_3|^2 a_3 \right) dt, \tag{12}
\end{aligned}$$

where  $d\xi$  is the complex white noise

$$\overline{d\xi} = 0, \quad \overline{d\xi^* d\xi} = dt, \quad \overline{d\xi d\xi} = 0. \quad (13)$$

Notice that compared to Eq. (9) in Eq. (12) we omitted the "self-energy" term proportional to  $g/N_0$ . This can be done as the oscillating factor  $\exp(-igt/N_0)$  can be absorbed into the noise Eq. (13) without changing its correlation properties.

Let us assume for a moment that there is no noise term in Eq. (12). Then Eq. (12) has a antisymmetric solution decoupled from the lossy site

$$\mathbf{a}_{\text{BIC}}(t) = e^{-igt} \begin{pmatrix} \sqrt{I} \\ 0 \\ -\sqrt{I} \end{pmatrix} \quad (14)$$

where intensity  $I$  can be linked to the mean population of the edge sites  $\bar{n}_{1,2} = IN_0 + 1/2$ . By examination of Eq. (12) one immediately identifies the three factors affecting the decay dynamics of this state:

(i) The stability of the BIC. If Eq.(14) is unstable, it can be destroyed by small perturbations.

(ii) The initial condition for solving Eq. (12). In more detail, we expect that the decay rate is dependent on how close the initial condition is to the symmetry protected BIC, Eq. (14). Moreover in establishing quantum to classical correspondence one can not deal with a single trajectory but with the ensemble of trajectories whose initial conditions are determined by the initial many-body quantum state of the system [24].

(iii) The noise term in Eq. (12) inversely proportional to  $\sqrt{N_0}$ . The noise can perturb even an intrinsically stable state driving it out of equilibrium. Notice that even though the reservoir does not supply particles into the system a stochastic driving force is still present in Eq. (12). Physically, this intrinsic noise is nothing but the quantum fluctuations arising from the noncommutativity of creation and annihilation operators. The noise term is important for the correct application of the pseudoclassical approach. For example, in the paradigm problem of the decaying quantum oscillator it ensures that the oscillator does not decay below its ground energy.

In the next section we discuss each of these factors in more detail.

### III. DECAY OF THE ANTISYMMETRIC STATE

#### A. Stability analysis

First we analyze the stability of the solution  $\mathbf{a}_{\text{BIC}}(t)$  for  $g \neq 0$ . Using the standard stability analysis [42] the stability of this solution can be examined by analyzing the matrix

$$\widehat{M} = \begin{pmatrix} gI & -J/2 & 0 & gI & 0 & 0 \\ -J/2 & -i\gamma/2 - gI & -J/2 & 0 & 0 & 0 \\ 0 & -J/2 & gI & 0 & 0 & gI \\ -gI & 0 & 0 & gI & J/2 & 0 \\ 0 & 0 & 0 & J/2 & -i\gamma/2 + gI & J/2 \\ 0 & 0 & -gI & 0 & J/2 & gI \end{pmatrix}. \quad (15)$$

If the imaginary part of all eigenvalues of  $\widehat{M}$  is non-positive, the BIC solution is stable. Fig. 1 (a) shows the imaginary parts of the eigenvalues as the function of  $gI$  for  $J = 1$  and  $\gamma = 0.4$ . It is seen that in this case the stability threshold corresponds to  $gI = 0.2$ . Above the threshold any tiny imbalance in the population of the edge sites will leads to excitation of the symmetric modes and the BIC loses its intensity. This process is exponential in time resulting in a rapid drop of intensity at the initial stage. However, once the stability threshold is crossed the solution  $\mathbf{a}_{\text{BIC}}(t)$  stabilizes at a certain value of intensity  $I_{\text{st}}$ ,

$$I_{\text{st}} = I_{\text{st}}(\gamma, g). \quad (16)$$

In what follows we shall refer to Eq. (16) as the stabilization level. We mention that, as expected, the stabilization level is approximately inversely proportional to  $g$  yet it is always smaller than the stability threshold deduced from Eq. (15). The described scenario is exemplified by thin solid lines in Fig. 2 (d, e) where, to provoke the symmetry breaking, we introduced a tiny population imbalance  $\sim 10^{-3}$  in the initial BIC state. The exponential decrease of intensity for  $g$  above the stability threshold and the effect of stabilization is clearly seen in the figure.

#### B. Quantum ensemble

Before simulating the decay of truly quantum states we have to introduce an ensemble classical initial condition corresponding to a quantum state loaded into the system. This,

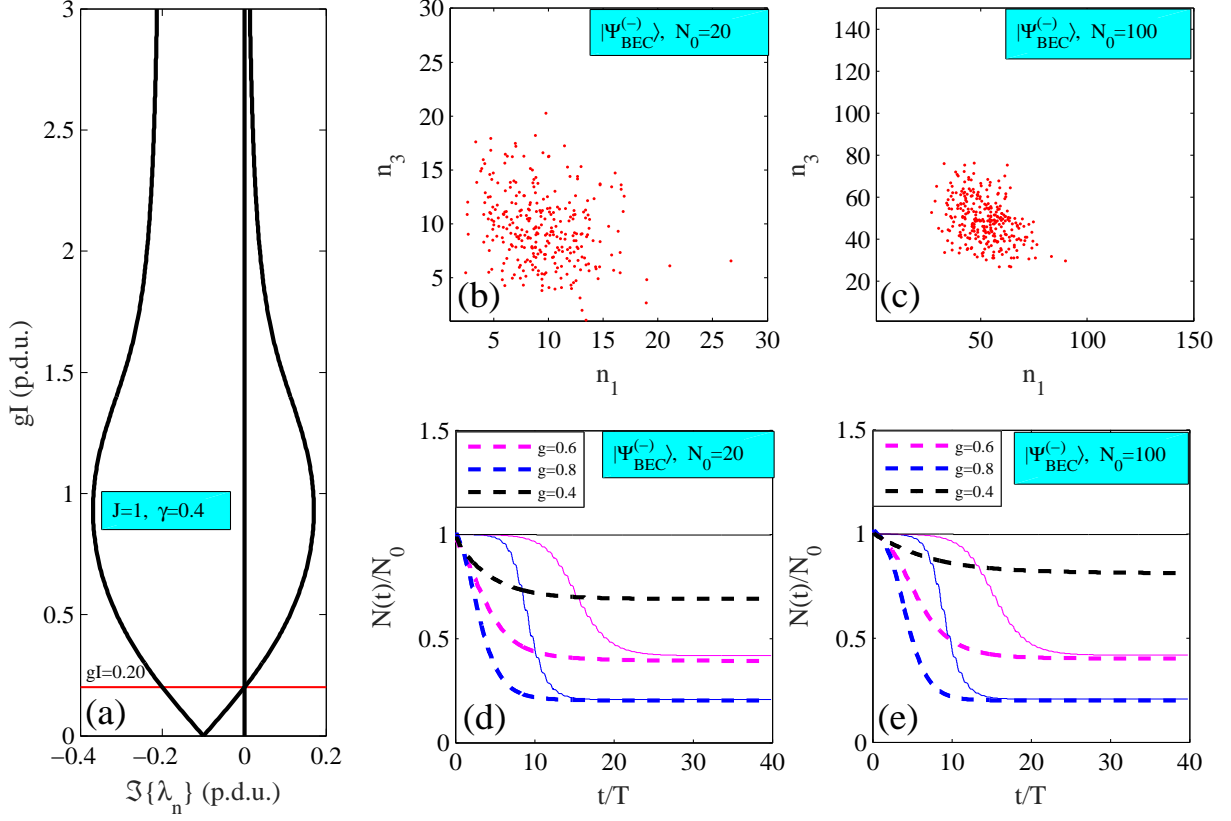


FIG. 2. (a) Imaginary parts  $\Im\{\lambda_n\}$  of eigenvalues of matrix Eq. (15) for  $\gamma = 0.4$ . (b, c) Initial conditions for the antisymmetric BEC in the space of populations of the first,  $n_1$  and the third,  $n_3$  sites for (b)  $N_0 = 20$  and (c)  $N_0 = 100$ . (d, e) Decay dynamics of the antisymmetric state with (d)  $N_0 = 20$  and (e)  $N_0 = 100$ . Thick dashed lines show the total number of particle against time for antisymmetric BEC initial conditions shown in subplot (d, c). Thin solid lines show the decay of the classical BIC state.

can be done by using the Husimi  $\mathcal{Q}$ -function,

$$\mathcal{Q}(\boldsymbol{\alpha}) = \frac{1}{\pi^3} \langle \boldsymbol{\alpha} | \hat{\mathcal{R}} | \boldsymbol{\alpha} \rangle, \quad (17)$$

where  $|\boldsymbol{\alpha}\rangle$  is the Glauber coherent state,

$$|\boldsymbol{\alpha}\rangle = e^{-\frac{|\alpha_1|^2 + |\alpha_2|^2 + |\alpha_3|^2}{2}} e^{\alpha_1 \hat{a}_1^\dagger + \alpha_2 \hat{a}_2^\dagger + \alpha_3 \hat{a}_3^\dagger} |\text{vac}\rangle \quad (18)$$

with  $\boldsymbol{\alpha} = \{\alpha_1, \alpha_2, \alpha_3\}$ . At first, for the initial state we choose an antisymmetric  $N$ -particle BEC. However, for the future convenience below we present a single formula for both sym-

metric,  $|\Psi_{\text{BEC}}^{(+)}\rangle$  and antisymmetric  $|\Psi_{\text{BEC}}^{(-)}\rangle$  condensates

$$|\Psi_{\text{BEC}}^{(\pm)}\rangle = \frac{1}{\sqrt{2^N N!}} \left( \hat{a}_1^\dagger \pm \hat{a}_3^\dagger \right)^N |\text{vac}\rangle. \quad (19)$$

After applying the Husimi transformation Eq. (17) one finds

$$\mathcal{Q}_{\text{BEC}}^{(\pm)}(\boldsymbol{\alpha}) = \frac{|\alpha_1 \pm \alpha_3|^{2N}}{\pi^3 2^N (N!)} e^{-|\alpha_1|^2 - |\alpha_2|^2 - |\alpha_3|^2}. \quad (20)$$

By applying the acceptance-rejection method [24] we generate the ensembles of the initial conditions according to the distribution function (20) for  $N_0 = 20$  and  $N_0 = 100$ , see panels (b) and (c) in Fig. 2, and then simulate the system dynamics. The result is depicted by the thick dashed lines in panels (d) and (e). Remarkably, in the unstable cases ( $g > 0.4$ ) we get the same fraction of bosons which is left in the system as it is predicted by the pure classical stability analysis given in the previous subsection. In the stable case  $g = 0.4$ , however, we observe essential deviations. These can be understood by noticing that every initial condition  $\mathbf{a}(t = 0)$  from the quantum ensemble is a superposition of the system linear eigenmodes,

$$\mathbf{b}_1 = \begin{pmatrix} \frac{1}{\sqrt{2}} \\ 0 \\ \frac{-1}{\sqrt{2}} \end{pmatrix}, \quad \mathbf{b}_2 = \begin{pmatrix} \frac{1}{2} \\ \frac{1}{\sqrt{2}} \\ \frac{1}{2} \end{pmatrix}, \quad \mathbf{b}_3 = \begin{pmatrix} \frac{1}{2} \\ \frac{-1}{\sqrt{2}} \\ \frac{1}{2} \end{pmatrix} \quad (21)$$

where the first eigenmode obviously corresponds to the symmetry protected BIC while the other two modes are coupled to the reservoir and decay within the characteristic time  $2\pi/\gamma$ . Thus, the solid and dashed lines in Fig. 2(d-e) may coincide only in the limit  $N_0 \rightarrow \infty$  where the quantum ensemble shrinks to the single point.

### C. The Role of the Noise

Now let us return to the Langevin dynamics governed by Eq. (12) where one could expect that even a stable antisymmetric BIC state Eq. (14) is subject to decay. To test this conjecture we solve numerically both the Langeven equation and the exact master equation, Eq. (2). The results are shown in Fig. 3. In Fig. 3(a) we depict the exact quantum solution for the total population. One can see that unlike the classical solutions in Fig. 2 the populations now continues to decay even after crossing the stabilization level. This decay is still exponential, however, with much smaller rate. In Fig. 3(b) we compare the population

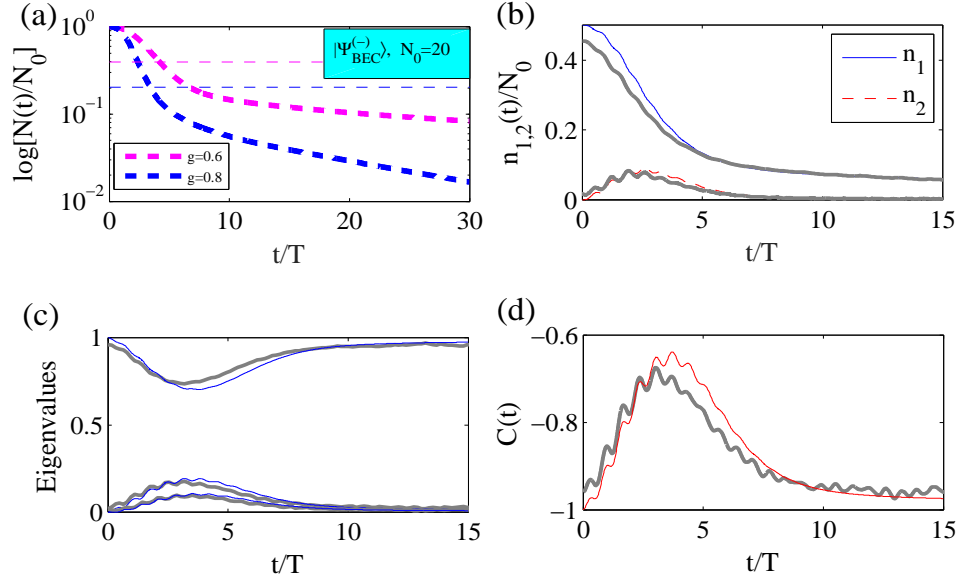


FIG. 3. Decay of the antisymmetric condensate for  $N_0 = 20$ . (a) Logarithmic plot of the full population against time obtained by solving the master equation Eq. (2). The thin dash lines show the stabilization levels from Fig. 2 (d). (b) Populations of the first and the second sites against time. Here and in the panels (c, d) thin lines are quantum simulations while thick grey lines are the results computed with the pseudoclassical approach,  $g = 0.8$ . (c) Normalized eigenvalues of the single particle density matrix Eq. (22),  $g = 0.8$ . (d) Correlation function Eq. (24),  $g = 0.8$ .

dynamics for the first and the second sites obtained by the pseudoclassical and quantum approaches. One can see that the two results are in a good agreement. This supports our conjecture that the noise destroys the classical symmetry protected BIC.

To look at the decay dynamics in more detail we compute the single particle density matrix  $\hat{\rho}$ , whose matrix elements are defined as

$$\rho_{\ell,\ell'} = \text{Tr} \left( \hat{a}_\ell^\dagger \hat{a}_{\ell'} \hat{\mathcal{R}} \right). \quad (22)$$

In the pseudoclassical framework this matrix corresponds to the correlation functions

$$\rho_{\ell,\ell'} = \langle a_\ell^* a_{\ell'} \rangle - \frac{1}{2} \delta_{\ell,\ell'}, \quad (23)$$

where the pointy brackets designate the ensemble average over Langevin trajectories. The single particle density matrix allows us to test whether the quantum state remains a BEC during the decay [43]. Namely, if all but one eigenvalues are zero the system is a condensate

state. Another related quantity is the correlation function [15],

$$C(t) = \frac{\rho_{1,3}}{\sqrt{\rho_{1,1}\rho_{3,3}}} = \frac{\langle a_1^* a_3 \rangle}{\sqrt{\langle |a_1|^2 \rangle \langle |a_3|^2 \rangle}}. \quad (24)$$

If  $C(t) = -1$  the system is an antisymmetric condensate and if  $C(t) = 1$ , then the condensate is symmetric. In Fig. 3 (c) we show the normalized eigenvalues of  $\hat{\rho}$ , while in Fig. 3 (d) we plotted the correlation functions, Eq. (24). Both subplots are consistent with the decay dynamics described above: First, the system rapidly departs from antisymmetric BEC. Then, after the stabilization level is crossed the system recoheres into antisymmetric BEC again and slowly decays as the metastable antisymmetric solution.

#### D. Symmetric BEC

To see the full picture in this section we also present results on the decay of symmetric BEC state, Eq. (19). One can see from Fig. 4 that in the course of evolution the symmetric BEC state rapidly drops intensity and decoheres into a fractional condensate with two non-zero eigenvalues of the single particle density matrix. Eventually, only a tiny fraction of the initial population survives after the system transits into a pure antisymmetric BEC well below the stability threshold. Again we see a good coincidence between the quantum and pseudoclassical results.

### IV. DECAY OF FRACTIONAL CONDENSATES

Next we examine the decay dynamics of fractional condensate states. The fractional condensate states are defined as those having more than one non-zero eigenvalues of the single particle density matrix [43]. The most obvious example of a fractional condensate is a Fock state

$$|\Psi_{\text{Fock}}\rangle = \frac{1}{(N/2)!} \left( \hat{a}_1^\dagger \hat{a}_3^\dagger \right)^{(N/2)} |\text{vac}\rangle, \quad (25)$$

where  $N_0/2$  particles occupy the first site and the rest  $N_0/2$  particle the third site. Directly applying Eq. (17) one finds

$$\mathcal{Q}_{\text{Fock}}(\boldsymbol{\alpha}) = \frac{|\alpha_1|^N |\alpha_3|^N}{\pi^3 [(N/2)!]^2} e^{-|\alpha_1|^2 - |\alpha_2|^2 - |\alpha_3|^2}. \quad (26)$$

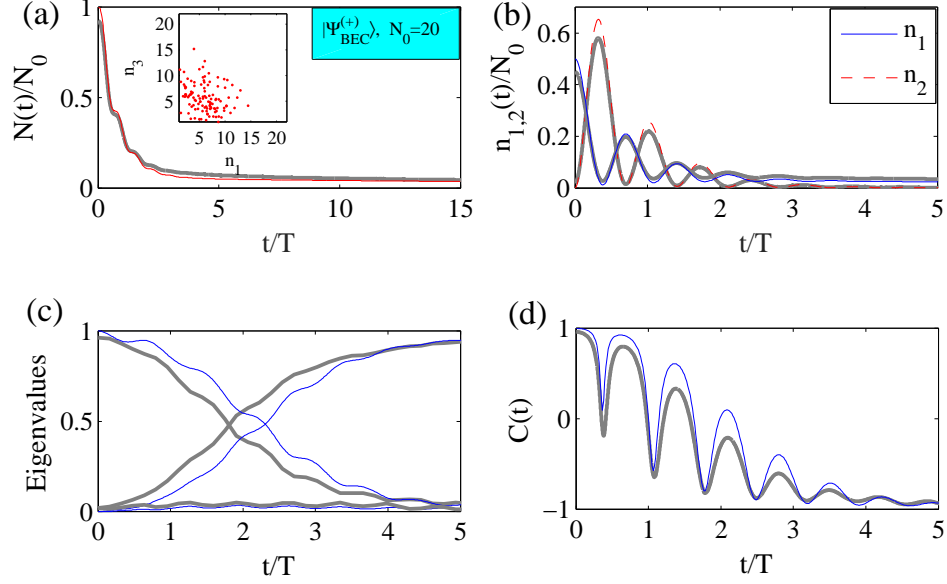


FIG. 4. Decay of symmetric condensate for  $g = 0.8$  and  $N_0 = 20$ . (a) The full population against time as obtained by solving the master equation Eq. (2). (b) Populations of the first and the second wells against time; thin line – quantum simulations, thick grey lines – pseudoclassical approach. (c) Normalized eigenvalues of the single particle density matrix Eq. (22). (d) Correlation function Eq. (24).

Another, less trivial, example is the (anti-)symmetric NOON state which is a Schrödinger cat state of  $N$  bosons in two wells,

$$|\Psi_{\text{NOON}}^{(\pm)}\rangle = \frac{1}{\sqrt{2(N!)}} \left[ (\hat{a}_1^\dagger)^N \pm (\hat{a}_3^\dagger)^N \right] |\text{vac}\rangle. \quad (27)$$

This state has the following  $\mathcal{Q}$ -function

$$\mathcal{Q}_{\text{NOON}}^{(\pm)}(\boldsymbol{\alpha}) = \frac{|\alpha_1|^{2N} + |\alpha_3|^{2N} \pm (\alpha_1 \alpha_3^*)^N \pm (\alpha_1^* \alpha_3)^N}{\pi^3 2(N!)} e^{-|\alpha_1|^2 - |\alpha_2|^2 - |\alpha_3|^2}. \quad (28)$$

In Fig. 5 we show the simulation results by both pure quantum and pseudoclassical approaches. One can see that despite the profound difference between the Fock state and the (anti-)symmetric NOON states clearly seen in insets in Fig. 5 (a-c), the decay dynamics is essentially identical. In all cases we see a rapid decay of a fractional state below the stability threshold after which the system recoheres to the antisymmetric BEC having lost the major part of the initial population. As before we see a good accuracy of the pseudoclassical approach.

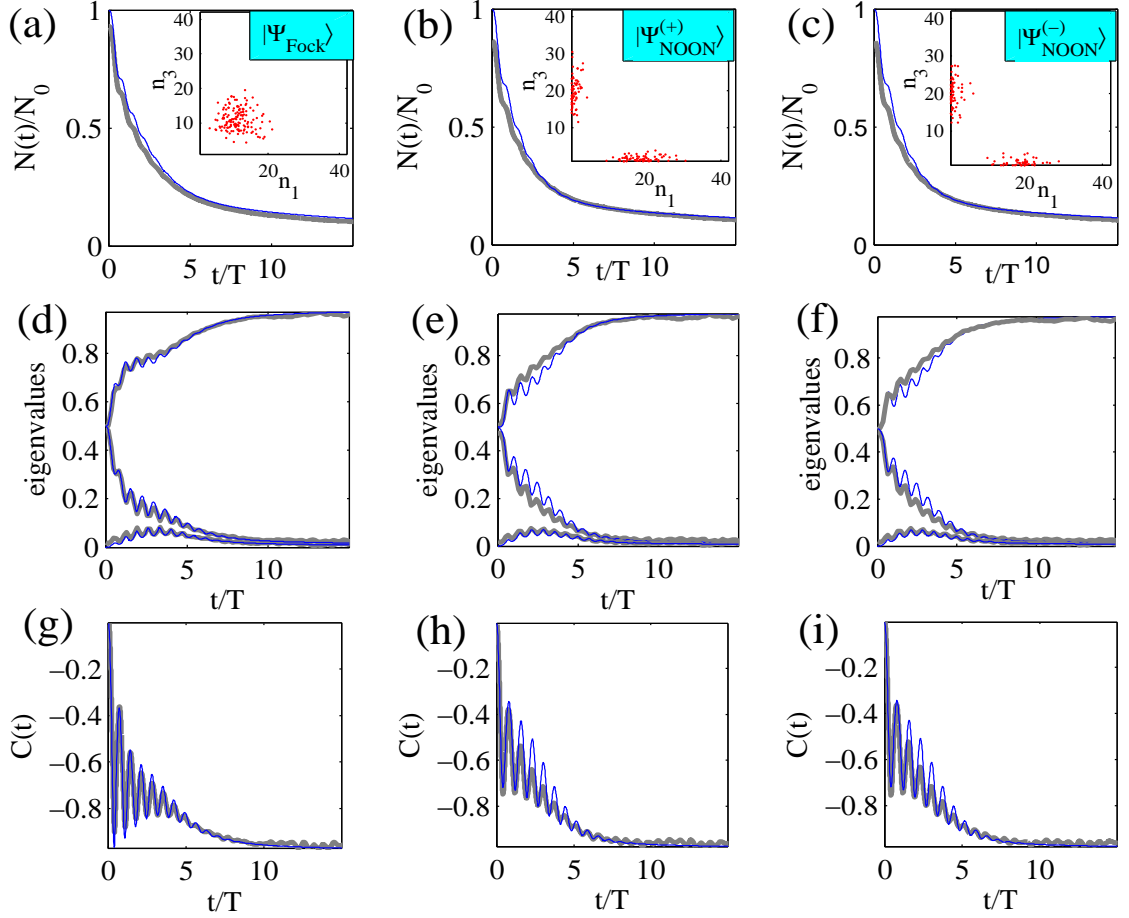


FIG. 5. Decay of fractional condensates,  $N_0 = 20$ ,  $T = 2\pi$  (p.d.u.); thick grey lines show the result by the pseudoclassical approach, thin blue - lines the solutions of the master equations. (a-c) Dynamics of the full population. The insets show the ensembles of initial conditions. (d-f) Normalized eigenvalues of the single particle density matrix for (d) Fock state, (e) symmetric NOON state, and (f) antisymmetric NOON state. (g-i) Correlation function, Eq. (24) for (g) Fock state, (h) symmetric NOON state, and (i) antisymmetric NOON state.

## V. SUMMARY AND CONCLUSION

We have examined the decay dynamics of quantum states with a definite number of bosons in three well open Bose-Hubbard model. It is demonstrate that the stability of the quantum state can be predicted from the classical perspective. The decay scenarios are drastically different depending on whether the solution is stable in the pseudoclassical limit.

In particular it is shown that in the pseudoclassical regime the antisymmetric BEC state is mapped to a symmetry protected bound state in the continuum (BIC). The BIC is only stable below a certain intensity threshold. Above the classical stability threshold the antisymmetric BEC rapidly decays and decoheres due to inter-particle interactions. Once the population has dropped below the threshold, however, the system recoheres to the antisymmetric BEC which decays at much slower rate due to the quantum fluctuations. It is demonstrated that the quantum fluctuations can be accurately described in the pseudoclassical framework by introducing a stochastic force with amplitude inversely proportional to the square root of the initial number of particles.

The pseudoclassical approach has been applied to several types of initial states with initial population only at the edge sites. Besides the antisymmetric BEC we have studied the decay of symmetric BEC, Fock, (anti-)symmetric NOON states. In all cases the initial bosonic cloud rapidly loses population to the reservoir and the decay can only slow down well below the classical stability threshold when the system recoheres to the metastable antisymmetric BEC. In all cases we observed a good coincidence between the numerical data obtained by the pseudoclassical approach and direct quantum simulations.

Recently, we have seen a surge of interest to decay dynamics of two-photon states [44–47]. We believe that the approach presented here provides the key to understanding the decay dynamics in the other solvable limit, namely, pseudoclassical regime. Finally, we would like to outline the future work ensuing from the present paper. It remains a question whether the asymptotic law of below threshold decay can be derived from the Langevin equations, Eq. (12) or the corresponding Fokker-Planck equation. We speculate that this problem may pose an interesting topic for future research.

This work has been supported by Russian Science Foundation through grant N19-12-00167. We appreciate discussions with A.F. Sadreev and E.N. Bulgakov. We are also grateful to G.P. Fedorov for his critical reading of the manuscript.

- 
- [1] S. Diehl, A. Micheli, A. Kantian, B. Kraus, H. P. Büchler, and P. Zoller, “Quantum states and phases in driven open quantum systems with cold atoms,” *Nature Physics* **4**, 878–883 (2008).

- [2] Y. Lin, J. P. Gaebler, F. Reiter, T. R. Tan, R. Bowler, A. S. Sørensen, D. Leibfried, and D. J. Wineland, “Dissipative production of a maximally entangled steady state of two quantum bits,” *Nature* **504**, 415–418 (2013).
- [3] F. Verstraete, M. M. Wolf, and J. I. Cirac, “Quantum computation and quantum-state engineering driven by dissipation,” *Nature Physics* **5**, 633–636 (2009).
- [4] D. Witthaut, F. Trimborn, and S. Wimberger, “Dissipation induced coherence of a two-mode Bose-Einstein condensate,” *Physical Review Letters* **101**, 200402 (2008).
- [5] T. Prosen and B. Žunkovič, “Exact solution of Markovian master equations for quadratic Fermi systems: thermal baths, open XY spin chains and non-equilibrium phase transition,” *New Journal of Physics* **12**, 025016 (2010).
- [6] P. Barmettler and C. Kollath, “Controllable manipulation and detection of local densities and bipartite entanglement in a quantum gas by a dissipative defect,” *Physical Review A* **84**, 041606 (2011).
- [7] J.-P. Brantut, J. Meineke, D. Stadler, S. Krinner, and T. Esslinger, “Conduction of ultracold fermions through a mesoscopic channel,” *Science* **337**, 1069–1071 (2012).
- [8] G. Barontini, R. Labouvie, F. Stubenrauch, A. Vogler, V. Guarrera, and H. Ott, “Controlling the dynamics of an open many-body quantum system with localized dissipation,” *Physical Review Letters* **110**, 035302 (2013).
- [9] S. Krinner, D. Stadler, D. Husmann, J.-P. Brantut, and T. Esslinger, “Observation of quantized conductance in neutral matter,” *Nature* **517**, 64–67 (2015).
- [10] M. Lebrat, P. Grišins, D. Husmann, S. Häusler, L. Corman, T. Giamarchi, J.-P. Brantut, and T. Esslinger, “Band and correlated insulators of cold fermions in a mesoscopic lattice,” *Physical Review X* **8**, 011053 (2018).
- [11] R. A. Pepino, J. Cooper, D. Meiser, D. Z. Anderson, and M. J. Holland, “Open quantum systems approach to atomtronics,” *Physical Review A* **82**, 013640 (2010).
- [12] A. Ivanov, G. Kordas, A. Komnik, and S. Wimberger, “Bosonic transport through a chain of quantum dots,” *The European Physical Journal B* **86**, 345 (2013).
- [13] A. R. Kolovsky, Z. Denis, and S. Wimberger, “Landauer-Büttiker equation for bosonic carriers,” *Physical Review A* **98**, 043623 (2018).
- [14] R. Labouvie, B. Santra, S. Heun, and H. Ott, “Bistability in a driven-dissipative superfluid,” *Physical Review Letters* **116**, 235302 (2016).

- [15] G. Kordas, D. Witthaut, and S. Wimberger, “Non-equilibrium dynamics in dissipative Bose-Hubbard chains,” *Annalen der Physik* **527**, 619–628 (2015).
- [16] K. Nemoto, C. A. Holmes, G. J. Milburn, and W. J. Munro, “Quantum dynamics of three coupled atomic Bose-Einstein condensates,” *Physical Review A* **63**, 013604 (2000).
- [17] R. Franzosi and V. Penna, “Self-trapping mechanisms in the dynamics of three coupled Bose-Einstein condensates,” *Physical Review A* **65**, 013601 (2001).
- [18] R. Franzosi and V. Penna, “Chaotic behavior, collective modes, and self-trapping in the dynamics of three coupled Bose-Einstein condensates,” *Physical Review E* **67**, 046227 (2003).
- [19] A. A. Bychek, P. S. Muraev, D. N. Maksimov, and A. R. Kolovsky, “Chaotic and regular dynamics in the three-site Bose-Hubbard model,” arXiv preprint arXiv:1910.12489 (2019).
- [20] K. W. Mahmud, H. Perry, and W. P. Reinhardt, “Quantum phase-space picture of Bose-Einstein condensates in a double well,” *Physical Review A* **71**, 023615 (2005).
- [21] S. Mossmann and C. Jung, “Semiclassical approach to Bose-Einstein condensates in a triple well potential,” *Physical Review A* **74**, 033601 (2006).
- [22] E. M. Graefe and H. J. Korsch, “Semiclassical quantization of an n-particle Bose-Hubbard model,” *Physical Review A* **76**, 032116 (2007).
- [23] F. Trimborn, D. Witthaut, and H. J. Korsch, “Exact number-conserving phase-space dynamics of the m-site Bose-Hubbard model,” *Physical Review A* **77**, 043631 (2008).
- [24] A. R. Kolovsky, H.-J. Korsch, and E.-M. Graefe, “Bloch oscillations of Bose-Einstein condensates: Quantum counterpart of dynamical instability,” *Physical Review A* **80**, 023617 (2009).
- [25] T. Zibold, E. Nicklas, C. Gross, and M. K. Oberthaler, “Classical bifurcation at the transition from Rabi to Josephson dynamics,” *Physical Review Letters* **105**, 204101 (2010).
- [26] A. A. Bychek, D. N. Maksimov, and A. R. Kolovsky, “NOON state of Bose atoms in the double-well potential via an excited-state quantum phase transition,” *Physical Review A* **97**, 063624 (2018).
- [27] A. A. Bychek, P. S. Muraev, and A. R. Kolovsky, “Probing quantum chaos in many-body quantum systems by the induced dissipation,” *Physical Review A* **100**, 013610 (2019).
- [28] A. A. Bychek, P. S. Muraev, D. N. Maksimov, and A. R. Kolovsky, “Open Bose-Hubbard chain: Pseudoclassical approach,” *Physical Review E* **101**, 012208 (2020).
- [29] Chia Wei Hsu, B. Zhen, A. D. Stone, J. D. Joannopoulos, and M. Soljačić, “Bound states in the continuum,” *Nature Reviews Materials* **1**, 16048 (2016).

- [30] E. Bulgakov, K. Pichugin, and A. Sadreev, “Light induced Josephson like current between two coupled nonlinear cavities coupled with a symmetrically positioned photonic crystal waveguide,” *Journal of Physics: Condensed Matter* **23**, 065304 (2011).
- [31] E. Bulgakov, K. Pichugin, and A. Sadreev, “Symmetry breaking for transmission in a photonic waveguide coupled with two off-channel nonlinear defects,” *Physical Review B* **83**, 045109 (2011).
- [32] M. Greiner, O. Mandel, T. Esslinger, T. W. Hänsch, and I. Bloch, “Quantum phase transition from a superfluid to a Mott insulator in a gas of ultracold atoms,” *nature* **415**, 39–44 (2002).
- [33] R. Gati and M. K. Oberthaler, “A bosonic Josephson junction,” *Journal of Physics B: Atomic, Molecular and Optical Physics* **40**, R61–R89 (2007).
- [34] J. Estève, C. Gross, A. Weller, S. Giovanazzi, and M. K. Oberthaler, “Squeezing and entanglement in a Bose-Einstein condensate,” *Nature* **455**, 1216–1219 (2008).
- [35] F. Meinert, M. J. Mark, E. Kirilov, K. Lauber, P. Weinmann, M. Gröbner, and H.-C. Nägerl, “Interaction-induced quantum phase revivals and evidence for the transition to the quantum chaotic regime in 1D atomic Bloch oscillations,” *Physical Review Letters* **112**, 193003 (2014).
- [36] C. J. Fujiwara, K. Singh, Z. A. Geiger, R. Senaratne, S. V. Rajagopal, M. Lipatov, and D. M. Weld, “Transport in Floquet-Bloch bands,” *Physical Review Letters* **122**, 010402 (2019).
- [37] R. Labouvie, B. Santra, S. Heun, S. Wimberger, and H. Ott, “Negative differential conductivity in an interacting quantum gas,” *Physical Review Letters* **115**, 050601 (2015).
- [38] A. Trenkwalder, G. Spagnolli, G. Semeghini, S. Coop, M. Landini, P. Castilho, L. Pezze, G. Modugno, M. Inguscio, A. Smerzi, and M. Fattori, “Quantum phase transitions with parity-symmetry breaking and hysteresis,” *Nature Physics* **12**, 826–829 (2016).
- [39] S. W. McDonald, “Phase-space representations of wave equations with applications to the eikonal approximation for short-wavelength waves,” *Physics Reports* **158**, 337–416 (1988).
- [40] K. Vogel and H. Risken, “Quantum-tunneling rates and stationary solutions in dispersive optical bistability,” *Physical Review A* **38**, 2409–2422 (1988).
- [41] D. Bortman and A. Ron, “Bistability in a quantum nonlinear oscillator,” *Physical Review A* **52**, 3316–3322 (1995).
- [42] A. J. Lichtenberg and M. A. Leiberman, *Regular and chaotic dynamics*, Vol. 38 (Springer Science & Business Media, 2013).
- [43] E. J. Mueller, T.-L. Ho, M. Ueda, and G. Baym, “Fragmentation of Bose-Einstein conden-

- sates,” *Physical Review A* **74**, 033612 (2006).
- [44] A. Crespi, L. Sansoni, G. Della Valle, A. Ciamei, R. Ramponi, F. Sciarrino, P. Mataloni, S. Longhi, and R. Osellame, “Particle statistics affects quantum decay and Fano interference,” *Physical Review Letters* **114**, 090201 (2015).
- [45] Hua Li Chen, G. Wang, and Ray Kuang Lee, “Nearly complete survival of an entangled biphoton through bound states in continuum in disordered photonic lattices,” *Optics Express* **26**, 33205 (2018).
- [46] Y.-X. Zhang, C. Yu, and K. Mølmer, “Subradiant bound dimer excited states of emitter chains coupled to a one dimensional waveguide,” *Physical Review Research* **2**, 013173 (2020).
- [47] A. N. Poddubny, “Quasiflat band enabling subradiant two-photon bound states,” *Physical Review A* **101**, 043845 (2020).